Final Report, Office of Naval Research
Grant N00014-99-1-0274, July 15 2002

Research Described in Proposal Entitled

Comparative Modeling and Analysis of Wideband Low-Frequency Acoustic Propagation in the Shallow Water Environment

James C. Preisig, Timothy F. Duda, and George V. Frisk
Applied Ocean Physics and Engineering Department, MS 11
Woods Hole Oceanographic Institution
Woods Hole, MA 02543
(508) 289-2736, jpreisig@whoi.edu, tduda@whoi.edu, gfrisk@whoi.edu

Abstract

This grant was supported by the Ocean Acoustics Program in the Sensors and Systems Division of the Ocean, Atmosphere and Space Department of ONR. This project was a direct follow-on, scientifically speaking, of research performed under Grant N00014-95-1-0029, "Analytical and numerical study of shallow-water acoustic mode coupling from solitary internal waves".

Modeling was done at frequencies of 50 to 2400 Hz in order to determine acoustic mode coupling behavior in shallow waveguides with a variety of basement properties. Modeling was done with a flat bottom, but this led to interesting but unphysical propagation properties at frequencies above 800 Hz. One mode with unphysically low bottom interaction existed at each modeled frequency. These modes will not persist in reality, so the runs needed to be repeated with a sloping bottom, stalling our progress. The FEPE parabolic equation code of NRL was initially used for modeling. To solve the problem we switched to the NRL RAM code and then modified it to enable simpler substitution of variable ocean waves, water depths, and bottom types.

The delay caused by this anomalous model behavior, while illuminating, has delayed interpretation and publication of our results. Further analysis of these effects is now underway under Grant N00014-01-1-0772, "Capturing uncertainty in the common tactical environmental picture".

Results

The basic result from our previous grant, which was that internal solitary waves and fronts cause significant and important mode coupling at 400 Hz acoustic signals, has been verified for a few coastal bottom types and at frequencies from 100 to 1000 Hz. The effect on 50 Hz signals is diminished. Influences at frequencies above 1000 Hz are now under investigation. Effects of variable bottom types bahave in a manner consistent with intuition. The numerical acoustic model results (simulations) have allowed us to validate the intuition and quantify the effect.

A publication is included, from the proceedings of the upcoming Sept. 2002 conference on littoral environmental variability, acoustics and sonar at the SACLANT Centre.

Presentations and Publications

T. F. Duda and J. C. Preisig, Signal coherence and energy effects of propagating internal solitary wave packets, Joint meeting of the Acoustical Society of America and the European Acoustics Association, Berlin, Germany, March 1999.

T. F. Duda, J. C. Preisig and G. V. Frisk, Studies of internal wave and bottom effects on broadband shallow-water propagation, 138th meeting of the Acoustical Society of America, Columbu, Ohio, November 1999.

T. F. Duda, Relative influences of various environmental factors on 50-1000 Hz sound propagation in shelf and slope areas, in *Proceedings of the conference "Impact of Littoral Environmental Variability on Acoustic Predictions and Sonar Performance"*, Kluwer, 2002.

RELATIVE INFLUENCES OF VARIOUS ENVIRONMENTAL FACTORS ON 50-1000 HZ SOUND PROPAGATION IN SHELF AND SLOPE AREAS

TIMOTHY F. DUDA

Applied Ocean Physics and Engineering Department- MS 11, Woods Hole Oceanographic Institution, Woods Hole MA 02543,USA

E-mail: tduda@whoi.edu

Within a given continental shelf or slope area acoustic propagation effects from many aspects of the environment sum to give the resultant total environmental effect on sound propagation. Signal parameters influenced by the environment include signal strength (transmission loss), vertical coherence scale, horizontal coherence scale, temporal coherence scale, and further signal details not measured by coherence scales, all as functions of frequency. Environmental (oceanographic) factors include but are not limited to bathymetric slope, episodic high-amplitude internal waves, continuous low-amplitude internal waves, seafloor attenuation, fronts, currents, source depth, and receiver depth. The effects of each of these environmental factors may be investigated individually with simulations or with specialized field experiments, but the results often can't be generalized because of first-order differences between regions. In many situations the various factors do not act independently, but are coupled, and not only do the individual parameters vary but their interactions may also change. An example from our previous work is the altered influence of mode-stripping (bottom interaction) in shallow water when high-amplitude internal waves are either present or absent. This effect is sensitive to source depth, bottom parameters, and wave parameters. This example and other simulated examples of differing dominant parameters at selected locations will be presented and compared with acoustic experiment data. **From** *Proceedings of the conference "Impact of Littoral Environmental Variability on Acoustic Predictions and Sonar Performance"*,

1 Introduction

Over the past decades many studies have examined acoustic field variability caused by fluctuating oceanographic conditions. Quite often these studies have focused on a single identifiable oceanographic process and have investigated its effects on sound propagation. This approach can effectively decipher and illuminate the physics of the interaction, but is an incomplete treatment of the complex oceanic system, where many competing geophysical processes can play a role simultaneously, and the where the total effect on sound may not be a simple summation of individual effects. Example studies and topics in the shallow water venue are McDaniel and McCammon [1], mode coupling and seabed properties; Shmelerv, Migulin and Petnikov [2], horizontal sound refraction by internal waves; Zhou, Zhang and Rogers [3], scattering and loss induced by groups of sinusoidal internal waves; Lynch *et al.* [4], perturbations from internal waves and tides near a polar front;

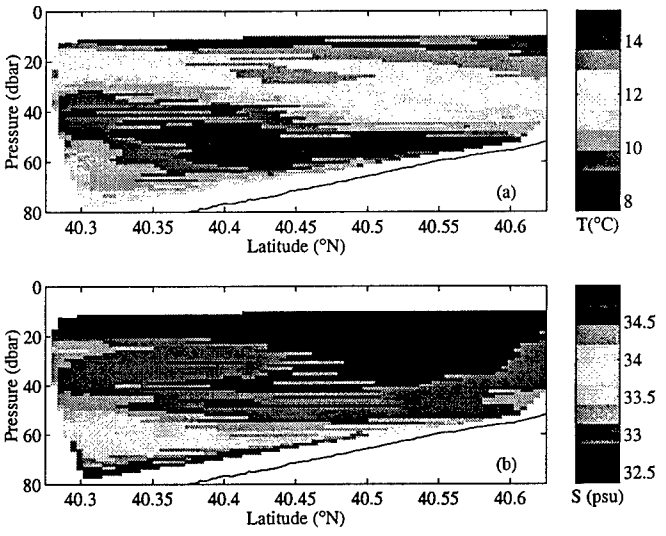

Figure 1. Temperature and salinity in one cross-shore south-to-north transect taken in the ONR Coastal Mixing and Optics Experiment in 1997. The water is warm at the surface, cooler below, and warm near the bottom. The salinity increases with depth in the south. The sound speed near the bottom in the warm salty slope water beneath the front is approximately 12 m/s greater than its minimum value in the water above. The figure is reproduced from published work [12].

Creamer [5], coupled mode and sub-bottom loss interaction; Preisig and Duda [6], individual sech^2-profile high-amplitude internal solitary waves; Tielbuerger, Finette and Wolf [7], propagation through internal waves in shallow water; Duda and Preisig [8], moving groups of sech^2 solitary waves; and Headrick et al. [9, 10], analysis and modeling of scattering by solitary waves in the SWARM experiment.

These and other rigorous studies of isolated processes, or at most a few processes, have advanced our understanding of shallow-water acoustics. On the other hand, making predictions of propagation and fluctuation behavior based on these studies is not simple. Many of the physical processes described by these studies arise only under specific conditions. Furthermore, the occurrence of one or more of these processes may eliminate the possibility of another taking effect. This possibility will be illustrated here with the example of the shelf/slope water front, a ubiquitous feature south of New England, altering the signal-level changing effect of mode coupling by internal solitary waves (ISWs). This example was motivated by observations of the front, appearing as salty and warm near-bottom layers in transects (Figure 1), and by computational studies of mode coupling by internal solitary waves. The coupling causes variable signal gain (or loss) because of variable energy exchange between modes as a function of wave location, and subsequently altered bottom interaction [6, 7, 8, 9, 10].

Some parameters and effects that must be considered in shallow water are listed here: Bathymetric slope, water mass fronts; internal solitary waves and packets; a quasi-stationary internal wave field; internal tides; surface tides; eddy structures; source depth; receiver depth; seabed layering; lateral seabed structure; and seabed material. The "relative influences" term in the title implies an attempt to order these in importance, but this

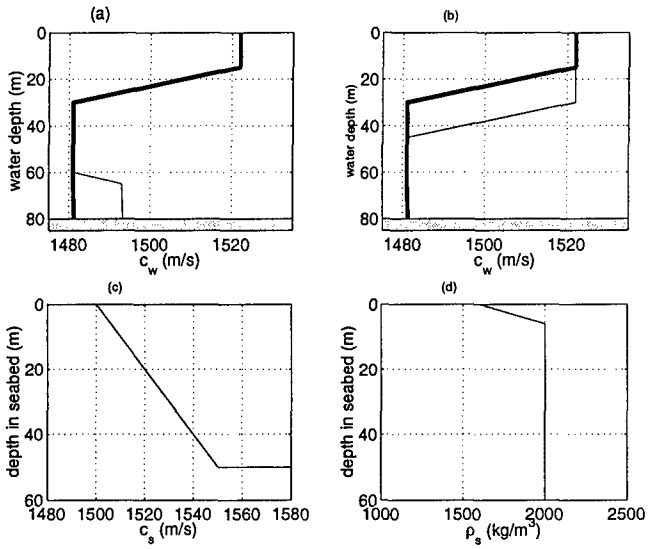

Figure 2. Sound speed and density parameters for the simulation are shown. (a) The background sound speed is shown with the thick line, and the perturbation of a deep warm layer is shown with the thin line. (b) The background sound speed is again shown with the thick line. The thin line shows a perturbed profile from a 15-m amplitude midwater pycnocline displacement, intended to mimic the effect of a 15-m amplitude internal wave of depression. (c) The sound speed in the seabed is shown. (d) The density structure in the seabed is shown.

is beyond the scope of this paper and may vary from place to place, which is entirely the issue.

Previous work [8] has pointed out some interacting parameters. For example, a packet of internal solitary waves was found to provide average signal gain for a shallow source but average signal attenuation for a deep source in the geometry that was considered. In addition, the position of internal waves relative to source and receiver was predicted to be of central importance in their ability to perturb acoustics [8, 10] and offers an explanation of effects observed in the SWARM experiment [10, 11]. Another paper in this volume lists additional interactions encountered in three WHOI experiments [11].

2 Computational Example

Interacting effects are illustrated with one computational example. The situation of a deep layer of warm salty water intruding onto the shelf, thereby perturbing signal loss effectiveness of an internal solitary wave packet, is studied using four computational runs. The runs include or exclude each of two water column sound speed structures: An internal solitary wave packet between 13 and 16 km from the sound source, and a warm layer below 60 m depth. Case 1 has no packet and no layer; Case 2 has the packet and no layer; Case 3 has no packet and the layer; Case 4 has both the packet and the layer. Cases 2 and 4 were run multiple times with variable packet location.

The background water sound speed (c_w) structure is shown in Figures 2a and 2b. An

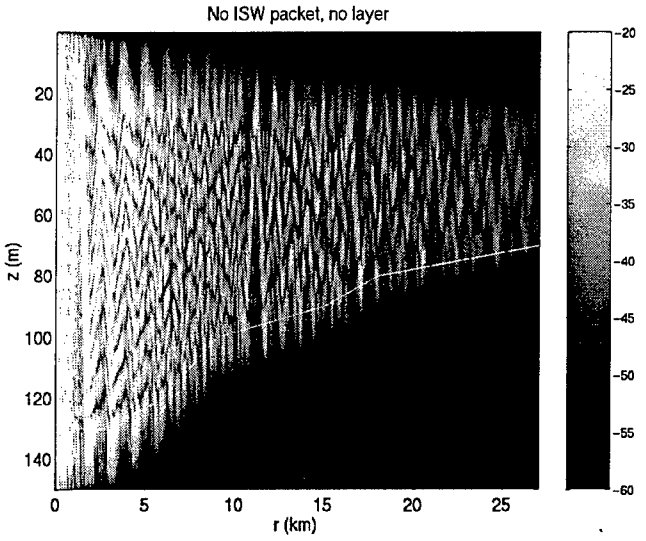

Figure 3. Transmission loss with cylindrical spreading removed (despread level) is plotted on a dB scale versus depth and range for the pycnocline-only situation (Case 1). Despread level is shown because it would not change systematically with range in the absence of sub-bottom loss, so any decreasing trend indicates bottom interaction. The RAM code was used to simulate a 400 Hz CW signal from a source at 20 m depth in 130-m deep water on the edge of the shelf. This is the "control" case of no ISW packet and no deep layer.

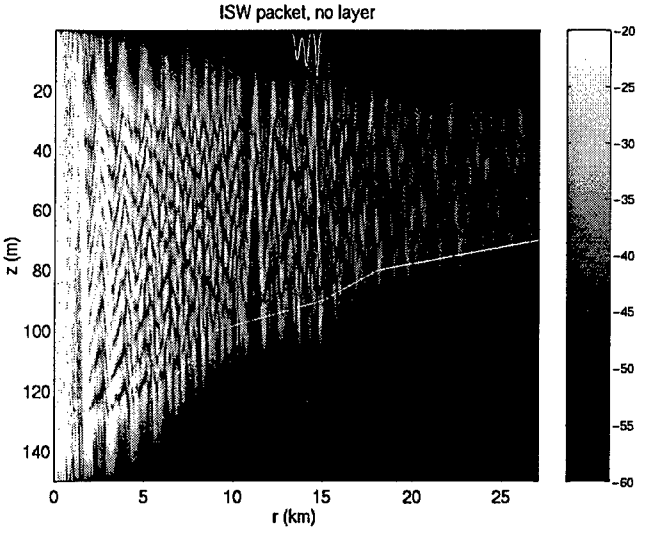

Figure 4. Despread level for a second PE simulation (Case 2) comparable to that depicted in the previous figure. The difference is the addition of an ISW packet of 15, 12 and 10 -m amplitude waves (shown schematically at the top) that couple energy into lossy high-order acoustic modes.

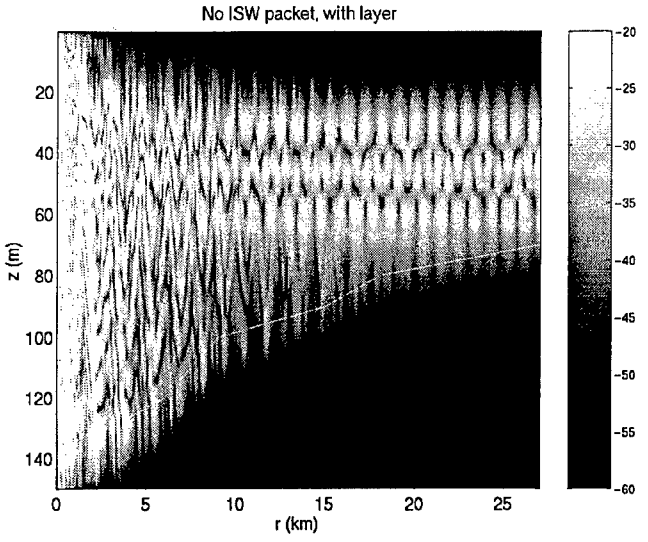

Figure 5. Despread level is shown for the Case 3 PE simulation. The water column has no ISW packet. The warm near-bottom layer is included. Levels are increased over Cases 1 and 2.

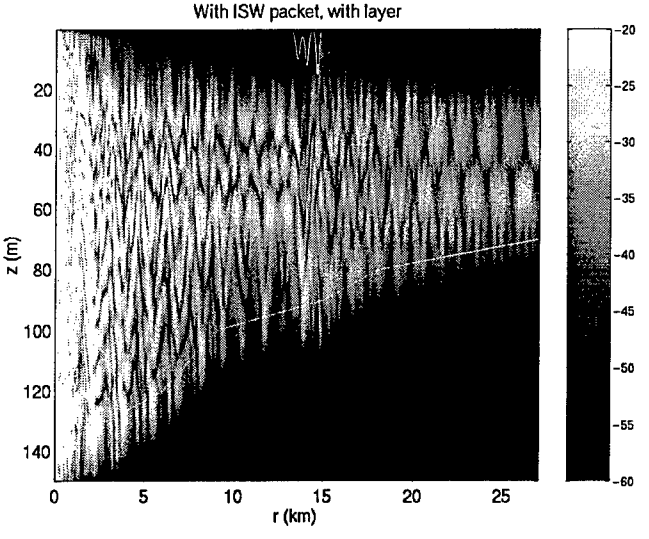

Figure 6. Despread level is shown for a fourth PE simulation (Case 4). The water column includes the ISW packet as does the Figure 4 case, and the the warm near-bottom layer shown in Figure 2.

upper layer of 1522 m/s transitions between 20 and 30 m depth to a deep layer of 1481 m/s. Below 65 m the sound speed increases linearly at a rate of 1 m/s per 65 m. The warm layer perturbation is shown in Figure 2a. It is a linear 12 m/s increase of c_w between 60 and 65 m depth, creating a sound channel. The effect of internal waves is displacement of the pycnocline (Figure 2b). The seabed structures are equal in all situations and are

uniform over range in a coordinate frame fixed to the local water/seabed boundary. Figure 2c shows the sound speed in the seabed c_s. It increases from 1500 m/s at the interface for 50 m at the rate of 1 s^{-1}, and increases below that to 2400 m/s at the next computational grid depth. This is intended to crudely imitate a mud and sand layer overlying bedrock. Figure 2d shows the density in the seabed, which increases linearly in the upper 6 meters and is constant beneath.

The RAM code [13] was used to solve the parabolic acoustic wave equation. The frequency was 400 Hz. The source was at 20 m depth in 130 m of water. The vertical depth increment was 0.25 meter and the range step was 1 meter. The input and output routines of the original code (RAM version 1.1) were modified: The bottom parameters were fixed with respect to range and were referenced into coordinates starting at the water/seabed boundary, and the complex acoustic field was output. Attenuation in the seafloor was 0.1 db per wavelength. Further parameters were c_0 = 1488 m/s and np = 2. ISW packet dimensions were as in previous work [8], with waves of 15, 12 and 10-m amplitude. Water depth, source depth, packet position and other parameters were chosen arbitrarily.

3 Discussion

The acoustic pressure magnitudes for each of the four situations are shown in Figures 3–7. The "despread level" is shown in order to eliminate the effect of cylindrical spreading and to highlight energy loss through sub-bottom interaction. Despread level is computed by multiplying the amplitude by the square root of the range before conversion to decibel.

The control case of no packet and no layer (Case 1, Figure 3) shows a gradual decline of energy with range and a gradual simplification of vertical acoustic field structure. This occurs because many modes are excited by the 20-m source and mode behavior is adiabatic. The higher order modes are subject to greater loss per km traveled than the lower order modes, creating this field structure that has only the bottom-hugging lower-order modes remaining after 15 km. The addition of an ISW packet at 13.5 km from the source causes modes to couple (Case 2, Figure 4). Only a few low modes are energized as the sound encounters the packet, and the randomizing effect on mode content causes the modal bandwidth to increase, sending energy upward in the water column. This effect is mentioned elsewhere in this volume [11], and is related to the "near receiver dominance" effect [9, 10, 11]. The newly-energized higher modes quickly dissipate downrange, leaving a depleted signal level relative to the control case (also mentioned in [11]). The precise blend of modes that are energized after the coupling is a sensitive function of packet location [8].

The inclusion of the warm layer below 60 m depth, a simple approach to model the effect of the front shown in Figure 1, yields essentially uniform despread level over range (averaged over mode interference patterns) at ranges greater than 10 km (Case 3, Figure 5). The few modes persisting to that range have little, if any, interaction with the bottom, in contrast with the attenuating modes of Figure 3. Including both the 13.5-km ISW packet and the layer (Case 4, Figure 6) reproduces the mode coupling behavior already seen in Figure 4. The high dB levels in Figures 3 and 4 also show how the layer serves to reduce sub-bottom loss of acoustic energy.

The ISW mode-coupling effect is seemingly the same with and without the layer, but it is not identical because the signal levels are reduced by different amounts in the two cases.

The examples shown are not sufficient to quantify the difference because the signal loss from packets is sensitive to packet position with a scale length of about a kilometer [8]. The position affects the coupling by controlling modal phases. Therefore Cases 2 and 4 were repeated for packet positions of 13 to 16 km from the source, at 50-m increments. Figure 7 shows the gain caused by packets. In the figure, Case 2 results are compared with Case 1 results and Case 4 results are compared with Case 3 results by plotting the ratios of acoustic energy in the water column at 27-km range. The ratio of energy is G_E. The result given by dividing levels shown in Figures 4 and 3 (-4.8 dB) is given by the large circle in Figure 7b. The result given by dividing levels shown in Figures 6 and 5 (-3.8 dB) is given by the large square. The Case 2 runs (no warm layer) give mean gain of about one, with high variability. This means that on average the bottom-loss sensitivity of the mode structure after encountering the packet is the same as before the packet. The Case 4 vs Case 3 ratios G_E are always less that one, averaging 0.31 (-5.1 dB). The explanation for the loss is that water-trapped modes dominate when the sound encounters the packet, so that mode coupling increases the mode bandwidth to include bottom-interacting modes, reducing energy at 27-km range.

Finally, adiabatic mode amplitudes vary with range over a longer scale of about 10 km, so packets near and far from the source will have different effects. Source depth also plays a role by controlling mode excitation. Therefore, this simple example must be examined in greater detail to firm-up the findings. Numerous other examples of interacting features deserve examination.

Acknowledgements

We thank the Office of Naval Research for supporting this research. Mike Collins wrote and distributed the RAM PE code used here in modified form. Jim Preisig and Jim Lynch have been continual collaborators in this work.

References

1. McDaniel, S. T. and D. F. McCammon, Mode coupling and the environmental sensitivity of shallow-water propagation loss predictions, *J. Acoust. Soc. Am.*, **82**, 217–223 (1987).
2. Shmelerv, A. Yu., A. A. Migulin and V. G. Petnikov Horizontal refraction of low frequency acoustic waves in the arents Sea stationary acoustic track experiment, *J. Acoust. Soc. Am.*, **92**, 1003–1007 (1992).
3. Zhou, J., X. Zhang and P. H. Rogers, Resonant interaction of sound wave with internal solitons in the coastal zone,*J. Acoust. Soc. Am.*, **90**, 2042–2054 (1991).
4. Lynch, J. F., J. Guoliang, R. Pawlowicz, D. Ray, A. J. Plueddemann, C.-S. Chiu, J. H. Miller, R. H. Bourke, A. R. Parsons and R. Muench, Acoustic travel-time perturbations due to shallow-water internal waves and internal tides in the Barents Sea Polar Front: Theory and experiment, *J. Acoust. Soc. Am.*, **99** 803–821 (1996).
5. Creamer, D. B., Scintillating shallow-water waveguides, *J. Acoust. Soc. Am.* **99**, 2825–2838 (1996).
6. Preisig, J. C. and T. F. Duda, Coupled acoustic mode propagation through continental-shelf internal solitary waves, *IEEE J. Oceanic Eng.*, **22**, 256–269 (1997).
7. Tielburger D., S. Finette and S. Wolf, Acoustic propagation through the internal wave field in a shallow water waveguide, *J. Acoust. Soc. Am.* **101**, 789–808 (1997).
8. Duda, T. F., and J. C. Preisig, A modeling study of acoustic propagation through moving

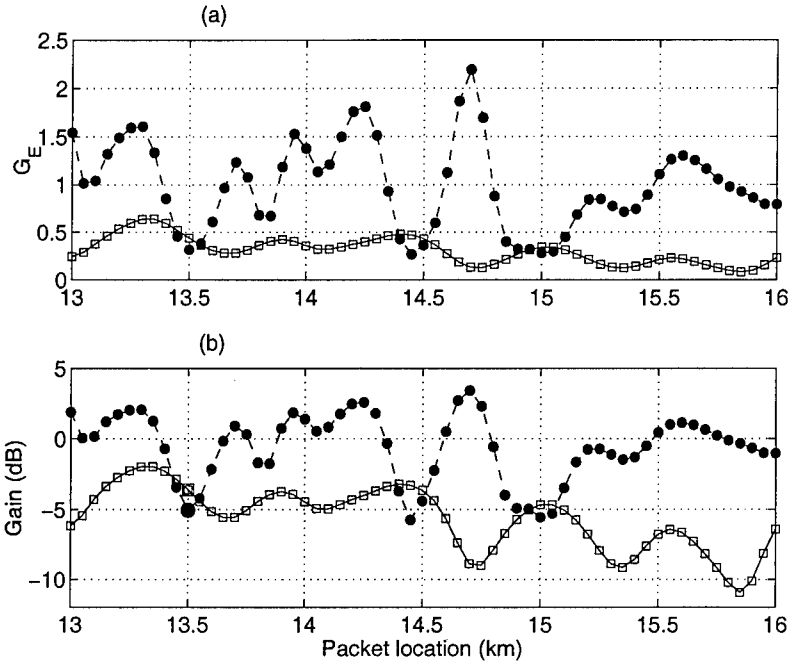

Figure 7. Gain caused by solitons is shown. (a) The filled circles show the ratio of energy in the water at 27 km range for multiple Case-2 runs to the energy of the Case-1 reference run, as a function of packet distance from the source (the only parameter that was varied between runs). The average gain in this case is close to one (0.99) with standard deviation 0.45. The open squares show the ratio of energy for multiple Case-4 runs to the Case 3 reference run. The average gain from the packets is 0.31 with standard deviation 0.14. (b) The data of (a) are shown on a dB scale. The mean Case 4 loss relative to Case 3 converts to -5.1 dB. The values for the computations shown in Figures 3–7, with packet at 13.5 km from the source, are shown with larger symbols.

shallow-water solitary wave packets, *IEEE J. Oceanic Eng.*, **24**, 16–32 (1999).

9. Headrick, R. H., J. F. Lynch, J. N. Kemp, A. E. Newhall, K. von der Heydt, J. Apel, M. Badiey, C.-S. Chiu, S. Finette, M. Orr, B. Pasewark, A. Turgut, S. Wolf, and D. Tielbuerger, Acoustic normal mode fluctuation statistics in the 1995 SWARM internal wave scattering experiment *J. Acoust. Soc. Am.* **107**, 201–220 (2000).
10. Headrick, R. H., J. F. Lynch, J. N. Kemp, A. E. Newhall, K. von der Heydt, J. Apel, M. Badiey, C.-S. Chiu, S. Finette, M. Orr, B. Pasewark, A. Turgut, S. Wolf, and D. Tielbuerger, Modeling mode arrivals in the 1995 SWARM experiment acoustic transmissions, *J. Acoust. Soc. Am.* **107**, 221–236 (2000).
11. Lynch, J., A. Fredricks, J. Colosi, G. Gawarkiewicz, A. Newhall, C.-S. Chiu amd M. Orr, Acoustic effects of environmental variability in the SWARM, PRIMER and ASIAEX experiments, this volume (2002).
12. Rehmann, C. R. and T. F. Duda, Diapycnal diffusivity inferred from scalar microstructure measurements near the New England shelf/slope front, *J. Phys. Oceanogr.*, **30**, 1354-1371 (2000).
13. Collins, M. D., Generalization of the split-step Padé solution, *J. Acoust. Soc. Am.* **92**, 382–385 (1993).

REPORT DOCUMENTATION PAGE

Form Approved
OMB No. 0704-0188

1. REPORT DATE *(DD-MM-YYYY)*	2. REPORT TYPE	3. DATES COVERED *(From – To)*
7/17/2002	Final Technical Report	1/1/99 – 12/31/01

4. TITLE AND SUBTITLE

Comparative Modeling and Analysis of Wideband Low-Frequency Acoustic Propagation in the Shallow Water Environment

5a. CONTRACT NUMBERS

5b. GRANT NUMBER
N00014-99-1-0274

5c. PROGRAM ELEMENT NUMBER

6. AUTHOR(S)

James C. Preisig, Timothy F. Duda , and George V. Frisk

5d. PROJECT NUMBER

5e. TASK NUMBER

5f. WORK UNIT NUMBER

7. PERFORMING ORGANIZATION NAME(S) AND ADDRESS(ES)

Woods Hole Oceanographic Institution
98 Water Street
Woods Hole, MA 02543

8. PERFORMING ORGANIZATION REPORT NUMBER

9. SPONSORING/MONITORING AGENCY NAME(S) AND ADDRESS(ES)

10. SPONSORING/MONITORING ACRONYM(S)

11. SPONSORING/MONITORING AGENCY REPORT NUMBER

12. DISTRIBUTION/AVAILABILITY STATEMENT

Approved for public release; distribution is unlimited

13. SUPPLEMENTARY NOTES

14. ABSTRACT

This grant was supported by the Ocean Acoustics Program in the Sensors and Systems Division of the Ocean, Atmosphere and Space Department of ONR. This project was a direct follow-on, scientifically speaking, of research performed under Grant N00014-95-1-0029, "Analytical and numerical study of shallow-water acoustic mode coupling from solitary internal waves".

Modeling was done at frequencies of 50 to 2400 Hz in order to determine acoustic mode coupling behavior in shallow waveguides with a variety of basement properties. Modeling was done with a flat bottom, but this led to interesting but unphysical propagation properties at frequencies above 800Hz. One mode with unphysically low bottom interaction existed at each modeled frequency. These modes will not persist in reality, so the runs needed to be repeated with a sloping bottom, stalling our progress. The FEPE parabolic equation code of NRL was initially used for modeling. To solve the problem we switched to the NRL RAM code and then modified it to enable simpler substitution of variable ocean waves, water depths, and bottom types.

The delay caused by this anomalous model behavior, while illuminating, had delayed interpretation and publication of our results. Further analysis of these effects is now underway under Grant N00014-01-1-0772, "Capturing uncertainty in the common tactical environmental picture".

15. SUBJECT TERMS

Acoustic Propagation; Broadband Modeling; Shallow-Water

16. SECURITY CLASSIFICATION OF:			17. LIMITATION OF ABSTRACT	18. NUMBER OF PAGES	19a. NAME OF RESPONSIBLE PERSON
a. REPORT	b. ABSTRACT	c. THIS PAGE			Timothy Duda
Unclassified	Unclassified	Unclassified	UL	9	19 b. TELEPHONE NUMBER *(Include are code)* 508-289-2495